Cell Stem Cell
Short Article

Lung Stem Cell Self-Renewal Relies on BMI1-Dependent Control of Expression at Imprinted Loci

Sima J. Zacharek,[1,3,5] Christine M. Fillmore,[1,3,5,11] Allison N. Lau,[1,3,5,11] David W. Gludish,[1,3,5,11] Alan Chou,[1,3,5] Joshua W.K. Ho,[4,6] Raffaella Zamponi,[1,3,5] Roi Gazit,[2,5] Christoph Bock,[5,7,8,9] Natalie Jäger,[5,7,8] Zachary D. Smith,[5,7,8] Tae-min Kim,[4] Arven H. Saunders,[1,3,5] Janice Wong,[1,3,5] Joo-Hyeon Lee,[1,3,5] Rebecca R. Roach,[1,3,5] Derrick J. Rossi,[2,5,8] Alex Meissner,[5,7,8] Alexander A. Gimelbrant,[3,10] Peter J. Park,[4,6] and Carla F. Kim[1,3,5,*]
[1]Stem Cell Program
[2]Immune Disease Institute, Program in Cellular and Molecular Medicine
Children's Hospital Boston, Boston, MA 02115 USA
[3]Department of Genetics
[4]Center for Biomedical Informatics
Harvard Medical School, Boston, MA 02115 USA
[5]Harvard Stem Cell Institute, Cambridge, MA 02138, USA
[6]Department of Medicine, Brigham & Women's Hospital, Boston, MA 02115 USA
[7]Broad Institute, Cambridge, MA 02142 USA
[8]Department of Stem Cell and Regenerative Biology, Harvard University, Cambridge, MA 02138 USA
[9]Max Planck Institute for Informatics, 66123 Saarbrücken, Germany
[10]Department of Cancer Biology, Dana Farber Cancer Institute, Boston, MA 02115 USA
[11]These authors contributed equally to this work
*Correspondence: carla.kim@childrens.harvard.edu
DOI 10.1016/j.stem.2011.07.007

SUMMARY

BMI1 is required for the self-renewal of stem cells in many tissues including the lung epithelial stem cells, Bronchioalveolar Stem Cells (BASCs). Imprinted genes, which exhibit expression from only the maternally or paternally inherited allele, are known to regulate developmental processes, but what their role is in adult cells remains a fundamental question. Many imprinted genes were derepressed in *Bmi1* knockout mice, and knockdown of *Cdkn1c* (*p57*) and other imprinted genes partially rescued the self-renewal defect of *Bmi1* mutant lung cells. Expression of p57 and other imprinted genes was required for lung cell self-renewal in culture and correlated with repair of lung epithelial cell injury in vivo. Our data suggest that BMI1-dependent regulation of expressed alleles at imprinted loci, distinct from imprinting per se, is required for control of lung stem cells. We anticipate that the regulation and function of imprinted genes is crucial for self-renewal in diverse adult tissue-specific stem cells.

INTRODUCTION

Many adult tissues including the lung maintain homeostasis or achieve injury repair via stem cell populations. In the distal murine lung, Clara cells, the bronchiolar nonciliated columnar epithelial cells, and alveolar type II cells (AT2) cells, the secretory epithelial cells in the alveolar space, have long been proposed to function as stem or progenitor cells. Clara cells are a self-maintaining cell population that gives rise to new Clara cells and ciliated cells during steady state lung homeostasis, demonstrating their role as adult progenitor cells (Rawlins et al., 2009). AT2 cells, similarly, are thought to function during development and after injury in adults as progenitors for the alveolar type I (AT1) cells that perform gas exchange. BASCs are an adult lung stem cell population that proliferates in response to distal lung cell injury when either Clara cell or AT1 cell damage occurs. BASCs may uniquely have bronchiolar and alveolar lineage potential as demonstrated by their ability to give rise to Clara and AT2 cells in culture, yet this activity remains to be shown in vivo (Kim et al., 2005). Ciliated cells undergo morphological changes after Clara cell injury in vivo, yet they do not directly contribute to lung repair and may be considered differentiated cells of the distal lung (Rawlins et al., 2007).

BMI1, a member of the Polycomb Repressive Complex 1 (PRC1), is required for the self-renewal of adult stem cells including BASCs (Dovey et al., 2008; Kim et al., 2005; Park et al., 2004; Sauvageau and Sauvageau, 2010). Serial plating of BASCs serves as an assay for measuring the self-renewal capacity of lung stem cells, and Bmi1-deficient BASCs exhibited little or no self-renewal. Furthermore, *Bmi1* knockout mice exhibited an impaired ability to repair Clara cell injury that was associated with failure of BASC expansion in vivo (Dovey et al., 2008). In the lung and other tissues, suppression of the *Cdkn2a* locus encoding p16/p19 is an important function of BMI1 that is required for stem cell self-renewal, yet this activity cannot account for the full range of BMI1 functions. Reducing levels of p16/p19 in *Bmi1* mutants in vivo or by knockdown in culture only partially rescued the BASC defects (Dovey et al., 2008), suggesting that other BMI1 target genes are important in controlling their self-renewal.

RESULTS

Imprinted Gene Derepression in *Bmi1*-Deficient Lung Cells

To test our hypothesis that additional targets of BMI1 are required for the self-renewal of lung stem cells, we compared gene expression profiles of FACS-purified cell populations from *Bmi1* wild-type and mutant lungs. As expected, multiple homeobox genes were derepressed in *Bmi1* mutant lung cells, as were *Cdkn2a* (*p16*/*p19*) and *Cdkn2b* (*p15*) (Figure 1A, Table S1 available online). Gene expression differences were validated by quantitative RT-PCR (qPCR) for 25 out of 30 genes examined (Figure 1B, Table S1). Other INK4 or CIP/KIP CDK inhibitor genes, including *Cdkn1a* (encoding p21) and *Cdkn1b* (encoding p27), were not differentially expressed (Figure 1B), even though *p21* is a BMI1 target in neural stem cells (Fasano et al., 2007). However, a different CIP/KIP family member, *Cdkn1c*, encoding p57 (referred to hereafter as p57 to designate gene or protein), was highly upregulated in *Bmi1* mutant lung cells (Figures 1A and 1B). p57 levels were 6.8- and 21.5-fold higher in *Bmi1* mutant cells compared to wild-type cells by microarray and qPCR, respectively ($p = 2.83e^{-4}$ and $p = 3.38e^{-13}$, respectively).

p57 belongs to another set of genes, previously known to be regulated by imprinting, that also demonstrated significant derepression in the *Bmi1* mutant cells. Importantly, imprinted genes were among the most highly dysregulated gene sets identified in the mutant cells using gene set enrichment analysis (GSEA Enrichment Score = 0.67, FDR $q < 0.001$) (Figure 1C, Table S2). Of the 84 imprinted genes (http://mousebook.org/catalog.php?catalog=imprinting) queried by microarray or qPCR, 33 were significantly dysregulated in *Bmi1* mutant lung cells (Figures 1B–1D, Table S1). Both maternally expressed genes (MEGs) and paternally expressed genes (PEGs) were significantly upregulated in *Bmi1* mutants (Figures 1A–1D).

A particularly interesting subset of imprinted genes, an imprinted gene network (IGN) that is transcriptionally downregulated during postnatal growth in several tissues including the lung and implicated in somatic growth control (Finkielstain et al., 2009; Gabory et al., 2009; Lui et al., 2008; Varrault et al., 2006), was derepressed in *Bmi1* mutant lung cells. For example, the IGN members *H19*, *Dlk1*, and *Igf2* were 5.8-, 3.4-, and 5.1-fold upregulated, respectively, in mutant cells by array, and increased expression was validated by qPCR (Figure 1D, Table S1). All of the IGN members we examined were significantly derepressed in the lung in the absence of *Bmi1*, including *p57*, *H19*, *Dlk1*, *Igf2*, *Plagl1*, *Grb10*, *Gtl2* (*Meg3*), *Mest*, *Ndn*, and *Peg3* (Figure 1D, Table S1).

We next determined the specificity of derepression of *p57* and other imprinted genes in the *Bmi1*-deficient lung stem cell compartment. There was no significant difference in the number of BASCs in wild-type and *Bmi1*-deficient lungs (data not shown and Dovey et al., 2008), ruling out gene expression differences caused by different BASC abundance. The CD31-negative, CD45-negative Sca-1-positive lung cell population typically used in self-renewal experiments contained BASCs and ciliated cells (Kim et al., 2005). We used an improved cell sorting strategy to further enrich each cell type on the basis of Sca-1, EPCAM, and CD24 abundance and further examine imprinted gene expression patterns. The CD31-negative, CD45-negative EPCAM-positive Sca-1-low, CD24-low distal lung cell population contains epithelial lung stem/progenitor cells and allows for further BASC enrichment, whereas the EPCAM-positive cells with high levels of CD24 are ciliated cells and the EPCAM-positive Sca-1-negative cells are AT2 cells (McQualter et al., 2010) (Figure S1 available online; data not shown). The IGN members *p57*, *Igf2*, and *Dlk1* were elevated in the more purified *Bmi1*-deficient BASCs (Figure 1E and data not shown). Importantly, *p57*, the most differentially expressed imprinted gene on our microarray list (Table S1), exhibited BASC-specific derepression; Bmi1 mutant BASCs had 1.7-fold more *p57* than their wild-type counterparts ($p = 0.05$), whereas there was no difference in the abundance of *p57* in ciliated cells or AT2 cells (relative to wild-type BASC levels set to 1, 2.4-fold mutant ciliated versus 3.9-fold wild-type ciliated, $p = 0.50$; and 0.30-fold mutant AT2 versus 0.43-fold wild-type AT2, $p = 0.50$) (Figure 1E).

Functional Analysis of Imprinted Genes in Lung Cell Self-Renewal

We used knockdown to determine that elevated imprinted gene expression levels contributed to the self-renewal defect of *Bmi1* mutant lung cells. Uninfected *Bmi1* mutant lung cells or those infected with negative control retrovirus rarely formed secondary colonies (Figure 2A, Dovey et al., 2008). Knockdown of *p57* in *Bmi1* mutant cells significantly reduced *p57* levels (Figure 2D, Figure S2) and increased secondary colony formation of *Bmi1* mutant cells (4.8% versus 0.7% from shEmpty control; $p = 0.09$; Figure 2A), although the difference was not statistically significant.

To test the idea that simultaneous dysregulation of imprinted genes caused self-renewal defects, we used a pooled shRNA approach to more substantially minimize imprinted gene overexpression in *Bmi1* mutant cells. Interestingly, small pools of shRNAs directed against MEGs (*p57*, *Grb10*, or *Ube3a*) or PEGs (*Igf2*, *Snrpn*, *Peg3*, or *Dlk1*) confirmed for knockdown activity (Figure S2) further improved secondary epithelial colony formation to 13% and 12%, respectively ($p = 0.008$ and $p = 0.001$). The most significant increase in *Bmi1* mutant secondary colonies was observed with a combined pool of MEG and PEG shRNAs (23%; $p = 2e^{-7}$; Figure 2A, Figure S2), consistent with the hypothesis that coordinated, BMI1-dependent regulation of imprinted genes is required for proper lung stem cell self-renewal.

Several of the imprinted genes for which combined knockdown rescued *Bmi1* mutant cells were also required for wild-type lung cell self-renewal. Virus expressing individual shRNAs for six different imprinted genes negatively impacted wild-type lung cell self-renewal (Figure 2B) (*p57*, *Grb10*, *Ube3a*, *Dlk1*, *Igf2*, and *Peg3*; p values compared to shEmpty are $2.9e^{-29}$, $1.6e^{-12}$, $1.6e^{-12}$, $1.6e^{-12}$, $3.4e^{-26}$, and $3.4e^{-17}$, respectively); *p57* and *Igf2* knockdown had the most significant impact on lung stem cell function. We confirmed a requirement for p57 in the self-renewal of wild-type lung cells using three different *p57* shRNAs (Figure 2C), which all effectively reduced *p57* expression levels (Figure S2). Individual shRNA for *Snrpn*, an imprinted gene that was not differentially expressed in *Bmi1*-deficient lung cells (Table S1), impaired self-renewal (67% secondary colony formation compared to 99% shEmpty, $p = 2.6e^{-6}$) (Figure 2B), although to a lesser extent than knockdown

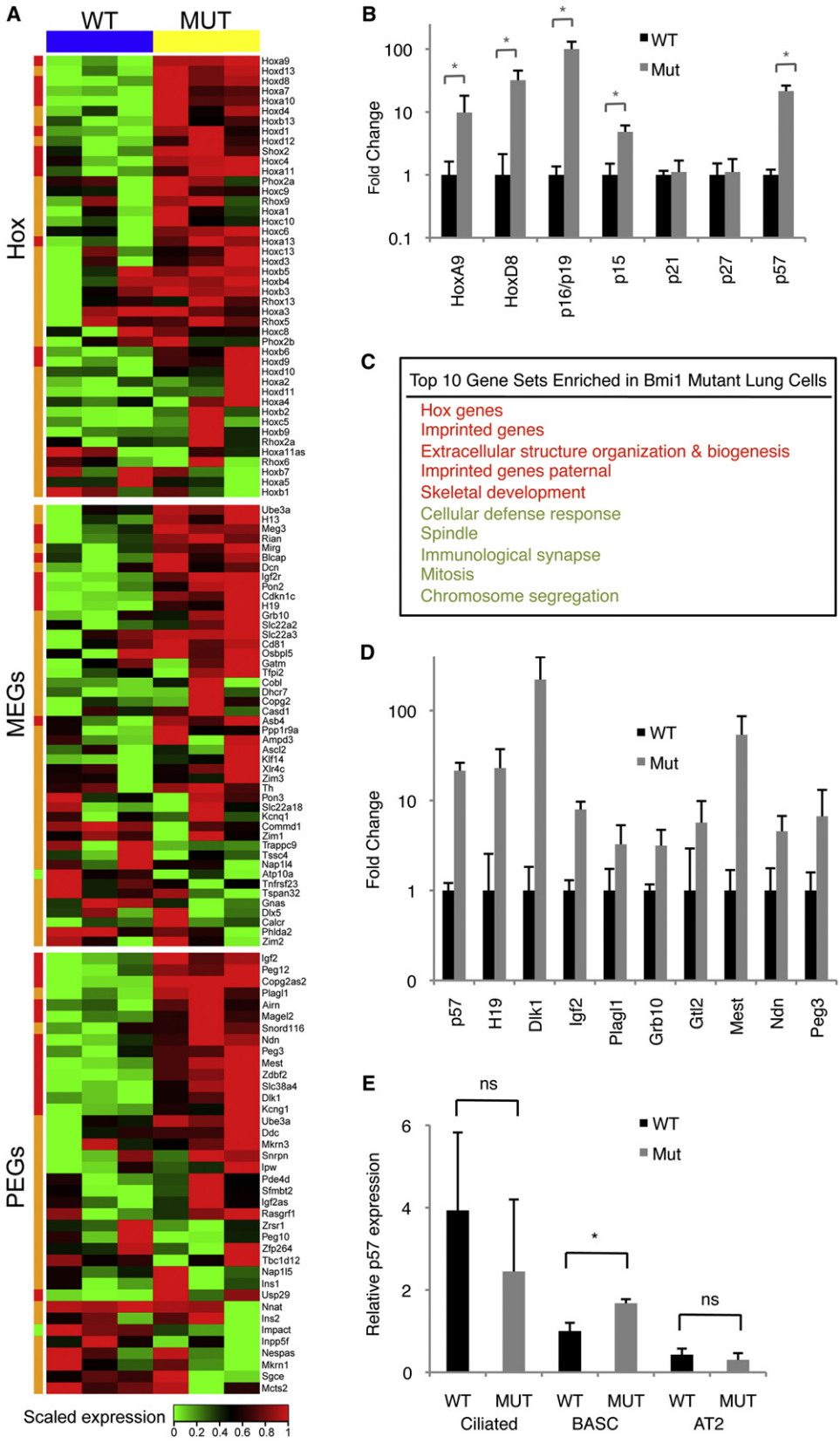
A
WT
MUT
Hox
MEGs
PEGs
Hoxa9
Hoxd13
Hoxd8
Hoxa7
Hoxa10
Hoxd4
Hoxb13
Hoxd1
Hoxd12
Shox2
Hoxc4
Hoxa11
Phox2a
Hoxc9
Rhox9
Hoxa1
Hoxc10
Hoxc6
Hoxa13
Hoxc13
Hoxd3
Hoxb5
Hoxb4
Hoxb3
Rhox13
Hoxa3
Rhox5
Hoxc8
Phox2b
Hoxb6
Hoxd9
Hoxd10
Hoxa2
Hoxd11
Hoxa4
Hoxb2
Hoxc5
Hoxb9
Rhox2a
Hoxa11as
Rhox6
Hoxb7
Hoxa5
Hoxb1
Ube3a
H13
Meg3
Rian
Mirg
Blcap
Dcn
Igf2r
Pon2
Cdkn1c
H19
Grb10
Slc22a2
Slc22a3
Cd81
Osbpl5
Gatm
Tfpi2
Cobl
Dhcr7
Copg2
Casd1
Asb4
Ppp1r9a
Ampd3
Ascl2
Klf14
Xlr4c
Zim3
Th
Pon3
Slc22a18
Kcnq1
Commd1
Zim1
Trappc9
Tssc4
Nap1l4
Atp10a
Tnfrsf23
Tspan32
Gnas
Dlx5
Calcr
Phlda2
Zim2
Igf2
Peg12
Copg2as2
Plagl1
Airn
Magel2
Snord116
Ndn
Peg3
Mest
Zdbf2
Slc38a4
Dlk1
Kcng1
Ube3a
Ddc
Mkrn3
Snrpn
Ipw
Pde4d
Sfmbt2
Igf2as
Rasgrf1
Zrsr1
Peg10
Zfp264
Tbc1d12
Nap1l5
Ins1
Usp29
Nnat
Ins2
Impact
Inpp5f
Nespas
Mkrn1
Sgce
Mcts2
Scaled expression
0 0.2 0.4 0.6 0.8 1
B
Fold Change
100
10
1
0.1
WT
Mut
HoxA9
HoxD8
p16/p19
p15
p21
p27
p57
C
Top 10 Gene Sets Enriched in Bmi1 Mutant Lung Cells
Hox genes
Imprinted genes
Extracellular structure organization & biogenesis
Imprinted genes paternal
Skeletal development
Cellular defense response
Spindle
Immunological synapse
Mitosis
Chromosome segregation
D
Fold Change
100
10
1
0
WT
Mut
p57
H19
Dlk1
Igf2
Plagl1
Grb10
Gtl2
Mest
Ndn
Peg3
E
Relative p57 expression
6
4
2
0
ns
*
ns
WT
Mut
WT MUT WT MUT WT MUT
Ciliated
BASC
AT2

of *p57* and other IGN members (e.g., 22% secondary colony formation; shp57). Similar results were seen with shRNA against *p27* (81% secondary colony formation, p = 0.00089), a nonimprinted p57 family member, whereas shRNA for the third nonimprinted p57 family member, *p21*, did not impair secondary colony formation (p = 0.12) (Figure 2B).

We directly compared *p57* gene expression levels after knockdown in mutant and wild-type cells (Figure 2D). Importantly, mutant lung cells infected with empty vector virus exhibited elevated levels of *p57* compared with equally treated wild-type cells, confirming the derepression of *p57* even in cultured, infected mutant cells. *p57* shRNA in mutant cells restored *p57* expression to wild-type control levels. Notably, *Bmi1*-deficient lung cells have elevated levels of many other imprinted genes, which also likely contributed to our inability to completely rescue secondary colony-forming ability solely with *p57* knockdown. *p57* shRNA in wild-type lung cells further reduced *p57* expression levels by 50% below normal wild-type levels, correlating with a reduction in secondary colony formation. Thus, increased p57 levels are incompatible with self-renewal, as are insufficient p57 levels. Together these data were consistent with the hypothesis that lung cell self-renewal relies on exquisite control of imprinted genes, perhaps particularly by function of the IGN (Varrault et al., 2006). Because *p57* exhibited more specific differential expression in BASCs than in other imprinted genes, we chose to further examine p57 regulation in vivo.

p57 Dynamic Expression in the Lung Injury Response

To further test the importance of p57 in lung stem cell function, we evaluated the normal expression patterns of p57 in vivo following lung injury with naphthalene, which is toxic to Clara cells, but not to BASCs (Kim et al., 2005). We performed four-color immunofluorescence analysis (IF) to score the incidence of Clara cells (CCSP-positive, SP-C-negative) and BASCs (CCSP-positive, SP-C-positive) with positive p57 staining at key time points during the course of lung injury repair (Figures 3A–3E, Figure S3A). The expression of p57 in lungs from mock-treated adult mice was relatively scarce, with expression restricted to BASCs and Clara cells (2.8% ± 5.6% and 1.3% ± 0.62%, respectively, of p57-positive cells), and most frequently found in ciliated cells (14.3% ± 3.9% of p57-positive cells) (Figures 3F and 3G, data not shown). As expected, 2 days following lung injury, most Clara cells were cleared from the airways, with only ciliated cells and BASCs persisting (Figure 3B; data not shown; Kim et al., 2005). The number of BASCs positive for p57 was lowest at this time point (none were detected), and there was a significant increase in p57-positive BASCs 3 days after naphthalene (6.1%, p = 0.04) that peaked after 5 days (21.8%, p = 0.01) (Figure 3F). Following the known pattern of BASC expansion and decline after appreciable repair of Clara cell injury (Kim et al., 2005), there was a rapid decline in p57-positive BASCs by day 7 after injury (2%, p = 0.01) (Figure 3F). The percentage of Clara cells with p57 similarly peaked at day 5 (18.5%, p = 0.006) and declined at day 7 after injury (5.1%, p = 0.02) (Figures 3D, 3E, and 3G). In contrast to BASCs and Clara cells, the incidence of ciliated cells (assessed with acetylated tubulin staining) with p57 expression was not different at days 5 and 7 after injury (Figure 3H). Thus, a dynamic pattern of p57 expression correlated with lung stem cell activity in vivo.

Bmi1 deficiency abrogated the normal dynamic pattern of p57 expression in lung stem cells after injury in vivo. The percentage of p57-positive BASCs and Clara cells in mutant and wild-type lungs was comparable 5 days after naphthalene (BASCS: 37.4% mutant versus 21.8% wild-type, p = 0.13; Claras: 21.7 mutant versus 18.5% wild-type, p = 0.57) (Figure 3H). However, p57-positive stem cell populations did not decline after naphthalene in *Bmi1* mutants (37.4% day 5 versus 39.77% day 7, p = 0.82 for mutant BASCs; and 21.7% day 5 versus 21.8% day 7, p = 0.99 for mutant Claras) (Figure 3J), and retained a significant increase relative to wild-type populations at day 7 (BASCs: 39.8% mutant versus 2% wild-type, p = 0.0004; Claras: 21.8% mutant versus 5.1% wild-type, p = 0.01) (Figure 3H). Importantly, the aberrant expression pattern of p57 was correlated with a significant deficiency in BASC expansion and Clara cell repair in *Bmi1* mutant lungs detectable at day 7 that persisted even 30 days after naphthalene treatment (Figure S3B; data not shown; Dovey et al., 2008). p57 expression in ciliated cells, the differentiated cells of the distal lung, was similar in wild-type and *Bmi1*-deficient lungs after naphthalene treatment (Figure 3H). These data suggested that BMI1 regulation of p57 is crucial in stem cells during lung injury repair in vivo.

BMI1-Dependent Regulation of Imprinted Loci

We next wished to determine the molecular nature of imprinted gene deregulation in *Bmi1* mutant cells. The monoallelic expression of imprinted genes is regulated by DNA methylation at maternal or paternal Differentially Methylated Regions (DMRs), many of which regulate the expression of imprinted genes in

Figure 1. Derepression of Imprinted Genes in *Bmi1* Mutant Lung Cells

(A) Gene expression differences of homeobox (Hox) genes, paternally expressed genes (PEGs), and maternally expressed genes (MEGs) from three samples each of *Bmi1* wild-type (WT) and mutant lung cells, as assessed by Affymetrix Mouse 430 2.0 gene expression microarray. Red indicates upregulated expression, green is downregulated expression, and differences with False Discovery Rate (FDR) < 0.1 are marked on the left of the heatmap (in red, upregulated; in green, downregulated).

(B) Validation of differential expression of homeobox genes and CDK inhibitors in *Bmi1* wild-type and mutant lung cells by qPCR. Expression from mutant samples (gray bars) is shown as fold change relative to wild-type samples (black bars) set to 1.

(C) Table showing the 10 gene sets revealed to be most overrepresented in *Bmi1* mutant samples using GSEA. Red, upregulated gene sets; green, downregulated gene sets.

(D) qPCR analysis of expression of imprinted gene network members in lung cells from wild-type (black bars) and mutant (gray bars) mice, normalized as in (B). The differential expression of all genes shown was statistically significant.

(E) Comparison of *p57* expression in wild-type (black bars) and mutant (gray bars) ciliated cells (EPCAM-positive, CD24-high), BASCs (EPCAM-positive, Sca-1-low, CD24-low) and AT2 cells (EPCAM-positive, Sca-1-negative, CD24-positive/negative). Asterisk (*) indicates $p \leq 0.05$. Error bars, standard deviation.

See also Tables S1 and S2 and Figure S1.

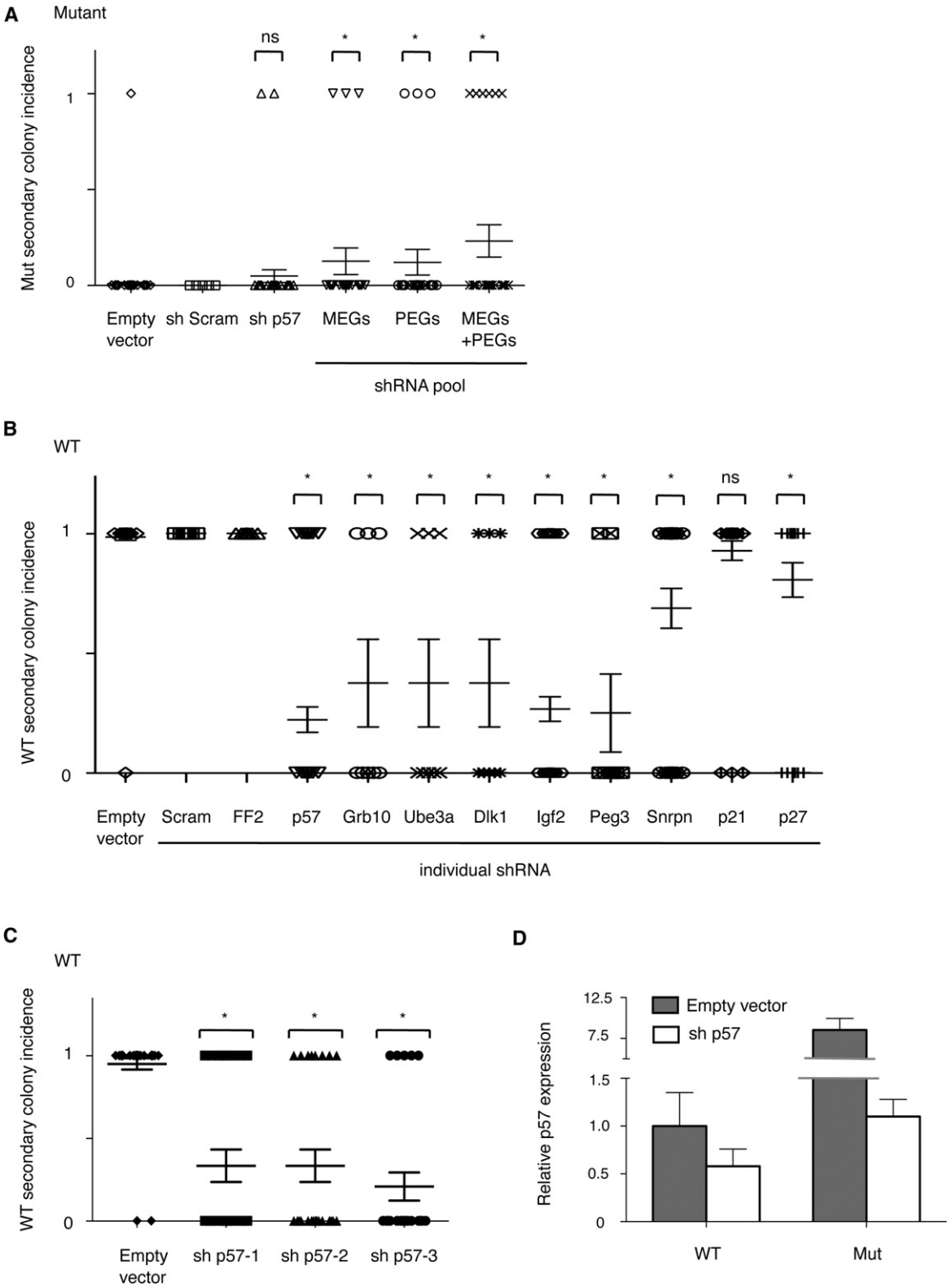

Figure 2. Lung Cell Self-Renewal in Culture Is Dependent on Precise Regulation of Imprinted Gene Expression

Formation of secondary colonies following knockdown of various imprinted genes in *Bmi1* mutant (A) or wild-type (B and C) lung cells by retroviral short hairpin RNA (shRNA) expression is shown. Each data point represents an individual well of primary colony cells plated for secondary colony formation, with 0 plotted for wells that lacked secondary colonies and 1 for wells with 1 or more secondary colonies. Infection with empty retroviral vector, sh-Scrambled (Scram), and sh-Firefly Luciferase (FF2) served as negative controls. Additional controls were *Snrpn*, *p21*, and *p27*. (A) Secondary colony formation in mutant cells infected with empty, Scram shRNA, or *p57* (sh2) shRNA; a MEG pool that included *p57* (sh3), *Grb10*, and *Ube3a* shRNAs; a PEG pool that included *Igf2*, *Snrpn*, *Peg3*, and *Dlk1* shRNAs; or a combined pool with all shRNAs (MEG + PEG) is shown. (B and C) Secondary colony formation in wild-type cells after infection with individual shRNA

clusters (Edwards and Ferguson-Smith, 2007). We confirmed that *p57* and *Gtl2* showed monoallelic, imprinted expression in wild-type BASCs (Figure S4A). To evaluate whether the derepressed expression of imprinted genes in *Bmi1* mutant lungs was due to loss of DNA methylation at DMRs, we performed reduced representation bisulfite sequencing (RRBS) (Gu et al., 2010) of *Bmi1* mutant and wild-type BASCs. A high degree of sequence coverage was achieved genome-wide in all samples, including the promoter regions of known imprinted genes and germline DMRs (not shown). DNA methylation levels at all DMRs and imprinted gene promoters from wild-type and *Bmi1* mutant cells were comparable (37.6% wild-type versus 40.5% mutant; $p = 0.57$ for DMRs and 28.3% versus 28.2%, $p = 0.99$ for promoters; Figure 4A). Methylation at individual imprinted gene germline DMRs examined was also similar, irrespective of whether most of the genes in the cluster or only some genes in the cluster showed derepression in mutants (Figure S4B).

We performed chromatin immunoprecipitation (ChIP) to assess the binding and activity of PRC1 components at imprinted loci. ChIP for the PRC1 component RING1B enriched for *p57*, *Dlk1*, and *Igf2* loci in wild-type lung cells similar to the positive control BMI1 target *p16* (Figure S4C). In *Bmi1* mutant lung cells, there was a modest decrease in RING1B enrichment for *p16*, *p57*, and *Dlk1* loci, but this change was only significant at *p57* ($p = 0.05$). Likewise, ChIP for the PRC1 catalytic mark, ubiquitinated histone H2A, enriched for all loci examined in wild-type lung samples, but enrichment in *Bmi1* mutant cells was only slightly decreased and did not change at *p57* (Figure S4C).

Finally, to evaluate whether BMI1-dependent regulation of imprinted loci occurs in a biallelic or monoallelic fashion, we modulated *Bmi1* levels in an SV40-transformed clonal mouse embryonic fibroblast (MEF) line derived from the F1 progeny of a Castaneus male and a 129 female (Gimelbrant et al., 2005). Using lentivirus to knock down *Bmi1* levels (Fasano et al., 2007), we observed an 80% reduction in *Bmi1* levels in shBmi1 MEFs compared with MEFs transduced with empty vector (Figure 4B). Importantly, the shBmi1 cells exhibited a 5.5-fold and a 4.5-fold increase in *p57* and *Igf2* expression, respectively ($p = 0.02$ and $p = 2e^{-5}$, respectively) (Figure 4C, Figure S4D), further confirming our findings in lung cells that BMI1 regulates imprinted gene expression. qPCR coupled with high resolution melt curve analysis (HRM) was used to differentiate between expression products derived from the maternal and paternal alleles with differential SNPs. The *p57* expression in F1 MEFs was primarily from the maternal *p57* allele, as expected for a MEG (Figure 4D, Figure S4D). In the shBmi1 cells, no shifts were observed in the HRM, indicating that imprinted gene expression remained derived from the maternal, expressed allele despite changes in overall *p57* expression levels (Figure 4D, Figure S4C). *Gtl2* exhibited a similar pattern of expression from the maternal, expressed allele in control and shBmi1 cells (not shown). Therefore, the increased expression of *p57* and other imprinted genes that occurs as a consequence of *Bmi1* deficiency is unlikely to be from loss of imprinting per se, and rather is a consequence of the dysregulation of the expressed allele at imprinted loci.

DISCUSSION

Our work shows that imprinted genes are important BMI1 targets in adult lung stem cells. Defects in cultured *Bmi1* mutant lung cells were attributable in part to derepression of imprinted genes, whereas insufficient levels of *p57* were also incompatible with wild-type lung stem cell self-renewal. Precise, dynamic control of p57 levels was observed during a time course of lung injury and repair in vivo. There was no evidence that *Bmi1* deficiency generally altered DNA methylation of imprinted loci, but instead BMI1 is implicated by our studies in the regulation of the expressed allele at these loci. Thus, an important mechanism for stem cell self-renewal is the control of expression levels of imprinted genes, providing an extra layer on top of typical imprinting mechanisms to regulate these critical loci.

Our results show that the PRC1 functions in imprinted gene regulation in adult stem cells. The Polycomb Repressive Complex 2 (PRC2) regulates imprinted gene repression in the placenta and early embryo at a small number of imprinted loci (Mager et al., 2003). In our studies, a much broader set of imprinted loci were overexpressed than observed in PRC2 or PRC1 mutant embryos (Mager et al., 2003; Terranova et al., 2008; Umlauf et al., 2004). DNA methylation was intact in *Bmi1* mutant adult lung cells, suggesting that imprinting mechanisms per se were not the cause of derepression of imprinted genes. Importantly, nongermline DMRs are associated with regulation of expression from imprinted loci (e.g., for *Igf2*; Feil et al., 1994 and Moore et al., 1997; for p57, Bhogal et al., 2004). We observed an increase in methylation at a silencing nongermline DMR in *Bmi1* mutants (Figure S4B), suggesting that BMI1-dependent changes in p57 expression do not rely on altered methylation. The nongermline regions regulating *Igf2* were not sufficiently covered in our RRBS data set. Therefore, we cannot rule out the possibility that nongermline DMRs or other differentially methylated sites were aberrant in *Bmi1* mutant lung cells and were partially responsible for changes in gene expression. On the other hand, our allelic expression analysis supports a role for BMI1 in regulation of the expressed allele at imprinted loci. Since we have not yet been able to ascertain direct binding of BMI1 at imprinted loci, the action of BMI1 in this context may be indirect. Alternatively, other direct modes of PRC1-dependent gene regulation, including chromatin compaction (Eskeland et al., 2010), may be essential for full repression of these loci. We suggest that the BMI1-dependent regulation of imprinted loci that is tied mechanistically to adult stem cell functions is distinct from the typical DNA methylation imprinting mechanisms that occur in development, adding another level of regulation to fine-tune control of the expressed allele at imprinted gene loci.

Our results demonstrate that a delicate, dynamic balance of expression from imprinted gene loci is needed for adult lung stem cell function. We have not yet confirmed that all of the imprinted genes we studied exhibit imprinted expression in BASCs with the exception of *p57* and *Gtl2*. *Slc22a3* and *Ube3a*, known to show tissue-specific imprinting, were predominantly

as indicated or three different shRNAs directed against p57. Results in (A), (B), and (C) are data from four, three, and three experiments, respectively. *$p < 0.05$. (D) qPCR analysis of knockdown efficiency of *p57* by sh3 in wild-type or *Bmi1* mutant lung cells; *p57* expression was measured relative to empty retrovirus control-infected wild-type cells. Error bars, standard error (A–C) or standard deviation (D). See also Figure S2.

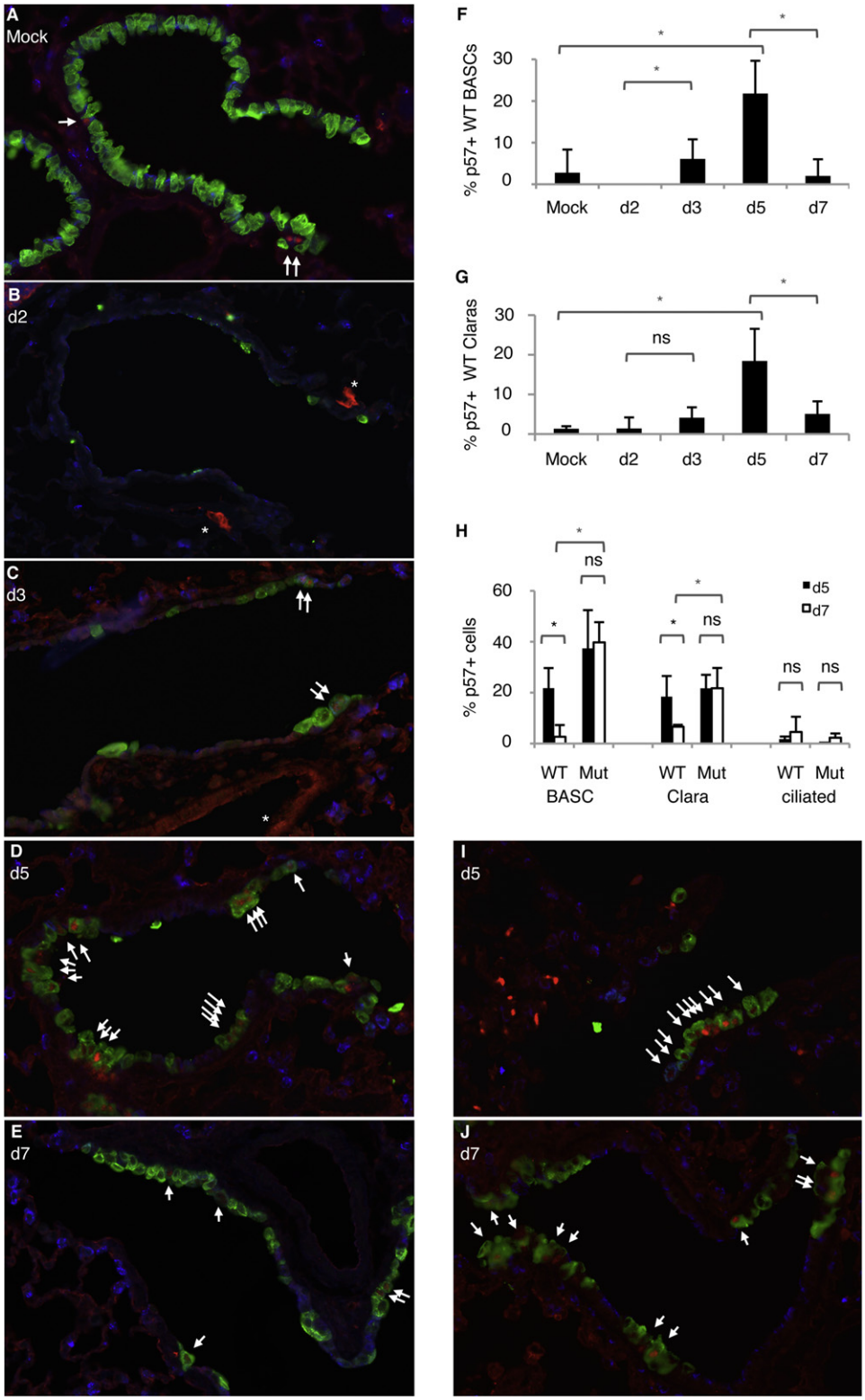

Figure 3. p57 Is Dynamically Regulated during Bronchiolar Cell Repair in Wild-Type Lung, but Not *Bmi1* Mutants

Sections were stained with antisera for p57 (red), SP-C (blue), and CCSP (green) along with DAPI (not shown), and four-color imaging was performed to score BASCs (CCSP-positive SP-C-positive) and Clara cells (CCSP-positive SP-C-negative). Ciliated cells were assessed by acetylated tubulin staining.

(A–E) Sections from wild-type lungs, isolated from vehicle-treated control mice (A, mock) or mice 2 (B), 3 (C), 5 (D), or 7 (E) days after treatment with naphthalene. For simplicity, only p57, CCSP, and SP-C staining are shown. Arrows, p57-positive Clara cells. (*), background red signal in red blood cells/blood vessels.

biallelically expressed in BASCs (Figure S4A), reinforcing the idea that BMI1 modifies the expression of this unique subset of genes independently of classic imprinting mechanisms. We focused on the effects of imprinted gene dysregulation in *Bmi1*-deficient BASCs, yet it is likely that other adult lung stem cell populations are impacted. Supporting this idea, we also observed dynamic expression of p57 during the naphthalene injury response in Clara cells, another lung stem/progenitor cell population. p57 levels fluctuated in stem cells during a time course of injury repair and high levels of p57 expression were incompatible with self-renewal whereas insufficient levels of p57 also prevented self-renewal. Therefore, the in vitro and in vivo data support a model in which there are important threshold levels of imprinted loci expression for stem cell function.

BMI1 regulation of both MEGs and PEGs, many of which are thought to operate in an IGN and which are also known to have growth-inhibiting and growth-promoting roles during development, respectively (Feil, 2009; Kelsey, 2007), was required for lung stem cell self-renewal. Findings related to the IGN are consistent with our results: the IGN similarly includes MEGs and PEGs (Varrault et al., 2006), manipulation of expression levels of individual IGN members has additive effects on expression levels of other IGN members (Gabory et al., 2009; Varrault et al., 2006), and changes in expression of the IGN with age in the lung and other tissues is not due to differential methylation (Lui et al., 2008). The IGN may function to provide an equilibrium between genes of opposing roles in order to facilitate growth control and development (Varrault et al., 2006), and we now link the IGN to stem cell function.

This work may implicate imprinted genes as self-renewal factors in diverse tissue-specific stem cells. Supporting this hypothesis, in a meta-analysis of public microarray data sets, the IGN was overrepresented in *Bmi1*-knockout lung cells, MEFs, cerebellum, and HSCs, yet not in *Bmi1*-deficient ESCs (Supplemental Information). p57 is a suggested mediator of HSC quiescence (Yamazaki et al., 2006), yet its function in stem/progenitor cells has only been shown during embryonic and early postnatal development (Bilodeau et al., 2009; Dugas et al., 2007; Dyer and Cepko, 2000; Georgia et al., 2006; Joseph et al., 2009; Mascarenhas et al., 2009; Park et al., 2005; Umemoto et al., 2006). PRC1 complex activity appears to be dispensable for self-renewal of ESCs, yet is required for silencing target genes important for cell fate decisions in ESC differentiation (Bernstein et al., 2007; Leeb et al., 2010). Interestingly, studies comparing ESCs and iPSCs further implicated an imprinted locus in the differentiation capacity of pluripotent cells (Liu et al., 2010; Stadtfeld et al., 2010). Therefore, the PRC complexes have separable functions in pluripotent, embryonic, and adult stem cells, with regulation of imprinted loci being a particularly crucial role of PRC1 in adult stem cell self-renewal.

EXPERIMENTAL PROCEDURES

Mice, Tissues, and Cells

Lung injury was performed as described (Dovey et al., 2008). Immunostaining was done with antisera for p57 (EP2515Y, Epitomics or Ab-3, Thermo Scientific), CCSP for Clara cells and BASCs (sc-25555, Santa Cruz), SP-C for AT2 cells and BASCs (sc-7705, Santa Cruz), and acetylated tubulin for ciliated cells (6-11B-1, Sigma-Aldrich). BASCs were scored as cells with individual nuclei positive for CCSP and SP-C. Primary lung cells were isolated from 6-week- to 4-month-old *Bmi1* wild-type or mutant mice and cultured as described (Dovey et al., 2008).

Retroviral Transduction of shRNA

shRNA sequences were cloned into MSCV-based retroviral vectors. Virus-containing media was concentrated, and primary cells were infected with polybrene 4 days after plating and resorted by FACS 3 days after infection, using GFP expression to select for infected cells.

Gene Expression Analysis

RNA was purified with Absolutely RNA purification kits (Agilent Technologies), amplified using the WT-Ovation Pico RNA Amplification System (Nugen), and analyzed using Affymetrix Mouse Genome 430 2.0 microarrays. qPCR was with TaqMan assays (Applied Biosystems) and a BioRad iQ5 Thermal Cycler with the housekeeping gene GAPDH for normalization.

Statistical Analysis

GraphPad Prism (GraphPad Software, Inc.) and Excel (Microsoft, Inc.) were used for graphing and statistical functions. p values were calculated using Student's t test, with $p < 0.05$ considered statistically significant.

ACCESSION NUMBERS

The GEO accession number for the microarray data reported in this paper is GSE30852.

SUPPLEMENTAL INFORMATION

Supplemental Information for this article includes two tables, four figures, and Supplemental Experimental Procedures and can be found with this article online at doi:10.1016/j.stem.2011.07.007.

ACKNOWLEDGMENTS

We thank Kim Lab members for discussions; S. Temple, C. Dulac, C. Gregg, D. Tenen, C. Hetherington, S. Elledge, J. Luo, N. Solimini, M. Hemann, C. Meacham, and B. Wilson for reagents and discussions; DFCI and CHB HemOnc FACS facilities; CHB Molecular Genetics Core facility; R. Bronson for histology; L. Zon, S. Orkin, and G. Daley for critical reading; and M. Goodell for sharing unpublished data. This work was supported by the Ladies Auxiliary to the Veterans of Foreign Wars (C.M.F.), the National Defense Science & Engineering Graduate Fellowship (A.N.L.), RO1 HL090136, U01 HL100402, American Cancer Society Research Scholar Grant #RSG-08-082-01-MGO, the V Foundation for Cancer Research, a Basil O'Conner March of Dimes Starter Award, and the Harvard Stem Cell Institute (C.F.K.).

Received: March 3, 2011
Revised: June 7, 2011
Accepted: July 14, 2011
Published: September 1, 2011

(F and G) Fluctuation in p57 levels in wild-type lungs at different time points after naphthalene treatment in BASCs (F) and Clara cells (G) was determined by four-color staining as described above.

(H) Quantification of BASCs, Clara cells, or ciliated cells positive for p57 in *Bmi1* mutant and wild-type lung cells at day 5 (d5, black bars) and day 7 (d7, white bars) following naphthalene-induced lung injury. Wild-type data are the same as shown in (F) and (G). *$p < 0.05$; ns = nonsignificant difference. Error bars, standard deviation.

(I and J) *Bmi1* mutant lungs 5 days (I) or 7 days (J) after naphthalene treatment were stained as in (A)–(E).

See also Figure S3.

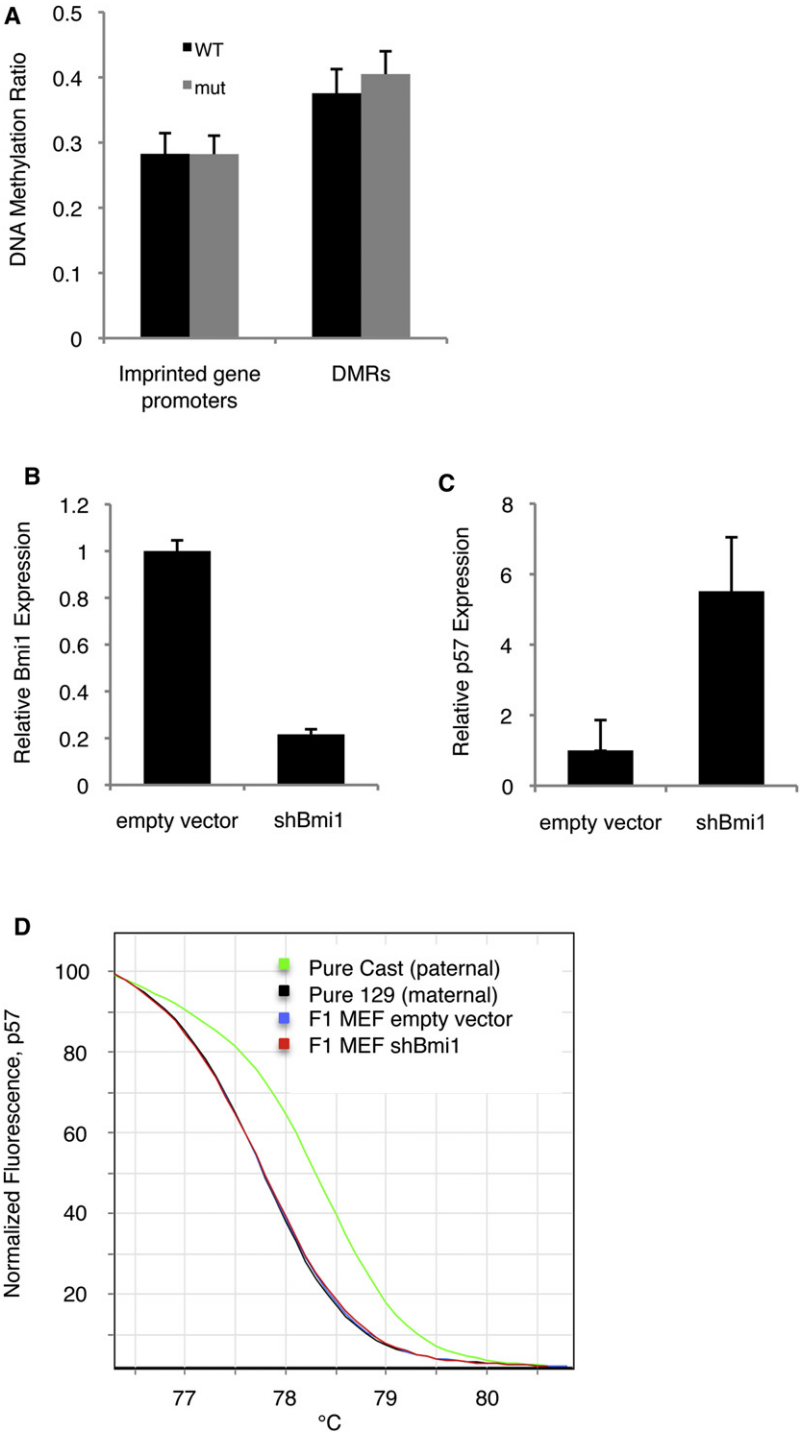

Figure 4. BMI1-Dependent Regulation of Imprinted Loci

(A) The average DNA methylation ratio was assessed in four independent biological replicates each of *Bmi1* wild-type and mutant BASCs by RRBS. The DNA methylation ratio was averaged across all wild-type (black bars) or *Bmi1* mutant (gray bars) imprinted gene promoter regions and DMRs; error bars represent standard errors for each pair.

(B–D) Modulation of *Bmi1* levels and high-resolution melt curve analysis (HRM) to determine allele-specific expression in F1 Cast/129 MEFs. Levels of *Bmi1* (B) and *p57* (C) after infection with lentivirus expressing shBmi1 are shown, relative to empty vector virus. HRM results (D) for *p57* showing expression from pure Cast cDNA (green, paternal imprinted allele control), pure 129 cDNA (black, maternal expressed allele control), empty virus-infected F1 MEFs (blue), and shBmi1 F1 MEFs (red) are shown. Values shown are the average of three replicates from a representative experiment.

See also Figure S4.

REFERENCES

Bernstein, B.E., Meissner, A., and Lander, E.S. (2007). The mammalian epigenome. Cell *128*, 669–681.

Bhogal, B., Arnaudo, A., Dymkowski, A., Best, A., and Davis, T.L. (2004). Methylation at mouse Cdkn1c is acquired during postimplantation development and functions to maintain imprinted expression. Genomics *84*, 961–970.

Bilodeau, S., Roussel-Gervais, A., and Drouin, J. (2009). Distinct developmental roles of cell cycle inhibitors p57Kip2 and p27Kip1 distinguish pituitary progenitor cell cycle exit from cell cycle reentry of differentiated cells. Mol. Cell. Biol. *29*, 1895–1908.

Dovey, J.S., Zacharek, S.J., Kim, C.F., and Lees, J.A. (2008). Bmi1 is critical for lung tumorigenesis and bronchioalveolar stem cell expansion. Proc. Natl. Acad. Sci. USA *105*, 11857–11862.

Dugas, J.C., Ibrahim, A., and Barres, B.A. (2007). A crucial role for p57(Kip2) in the intracellular timer that controls oligodendrocyte differentiation. J. Neurosci. *27*, 6185–6196.

Dyer, M.A., and Cepko, C.L. (2000). p57(Kip2) regulates progenitor cell proliferation and amacrine interneuron development in the mouse retina. Development *127*, 3593–3605.

Edwards, C.A., and Ferguson-Smith, A.C. (2007). Mechanisms regulating imprinted genes in clusters. Curr. Opin. Cell Biol. *19*, 281–289.

Eskeland, R., Leeb, M., Grimes, G.R., Kress, C., Boyle, S., Sproul, D., Gilbert, N., Fan, Y., Skoultchi, A.I., Wutz, A., and Bickmore, W.A. (2010). Ring1B compacts chromatin structure and represses gene expression independent of histone ubiquitination. Mol. Cell *38*, 452–464.

Fasano, C.A., Dimos, J.T., Ivanova, N.B., Lowry, N., Lemischka, I.R., and Temple, S. (2007). shRNA knockdown of Bmi-1 reveals a critical role for p21-Rb pathway in NSC self-renewal during development. Cell Stem Cell *1*, 87–99.

Feil, R. (2009). Epigenetic asymmetry in the zygote and mammalian development. Int. J. Dev. Biol. *53*, 191–201.

Feil, R., Walter, J., Allen, N.D., and Reik, W. (1994). Developmental control of allelic methylation in the imprinted mouse Igf2 and H19 genes. Development *120*, 2933–2943.

Finkielstain, G.P., Forcinito, P., Lui, J.C., Barnes, K.M., Marino, R., Makaroun, S., Nguyen, V., Lazarus, J.E., Nilsson, O., and Baron, J. (2009). An extensive genetic program occurring during postnatal growth in multiple tissues. Endocrinology *150*, 1791–1800.

Gabory, A., Ripoche, M.A., Le Digarcher, A., Watrin, F., Ziyyat, A., Forné, T., Jammes, H., Ainscough, J.F., Surani, M.A., Journot, L., and Dandolo, L. (2009). H19 acts as a trans regulator of the imprinted gene network controlling growth in mice. Development *136*, 3413–3421.

Georgia, S., Soliz, R., Li, M., Zhang, P., and Bhushan, A. (2006). p57 and Hes1 coordinate cell cycle exit with self-renewal of pancreatic progenitors. Dev. Biol. *298*, 22–31.

Gimelbrant, A.A., Ensminger, A.W., Qi, P., Zucker, J., and Chess, A. (2005). Monoallelic expression and asynchronous replication of p120 catenin in mouse and human cells. J. Biol. Chem. *280*, 1354–1359.

Gu, H., Bock, C., Mikkelsen, T.S., Jäger, N., Smith, Z.D., Tomazou, E., Gnirke, A., Lander, E.S., and Meissner, A. (2010). Genome-scale DNA methylation mapping of clinical samples at single-nucleotide resolution. Nat. Methods *7*, 133–136.

Joseph, B., Andersson, E.R., Vlachos, P., Södersten, E., Liu, L., Teixeira, A.I., and Hermanson, O. (2009). p57Kip2 is a repressor of Mash1 activity and neuronal differentiation in neural stem cells. Cell Death Differ. *16*, 1256–1265.

Kelsey, G. (2007). Genomic imprinting–roles and regulation in development. Endocr. Dev. *12*, 99–112.

Kim, C.F., Jackson, E.L., Woolfenden, A.E., Lawrence, S., Babar, I., Vogel, S., Crowley, D., Bronson, R.T., and Jacks, T. (2005). Identification of bronchioalveolar stem cells in normal lung and lung cancer. Cell *121*, 823–835.

Leeb, M., Pasini, D., Novatchkova, M., Jaritz, M., Helin, K., and Wutz, A. (2010). Polycomb complexes act redundantly to repress genomic repeats and genes. Genes Dev. *24*, 265–276.

Liu, L., Luo, G.Z., Yang, W., Zhao, X., Zheng, Q., Lv, Z., Li, W., Wu, H.J., Wang, L., Wang, X.J., and Zhou, Q. (2010). Activation of the imprinted Dlk1-Dio3 region correlates with pluripotency levels of mouse stem cells. J. Biol. Chem. *285*, 19483–19490.

Lui, J.C., Finkielstain, G.P., Barnes, K.M., and Baron, J. (2008). An imprinted gene network that controls mammalian somatic growth is down-regulated during postnatal growth deceleration in multiple organs. Am. J. Physiol. Regul. Integr. Comp. Physiol. *295*, R189–R196.

Mager, J., Montgomery, N.D., de Villena, F.P., and Magnuson, T. (2003). Genome imprinting regulated by the mouse Polycomb group protein Eed. Nat. Genet. *33*, 502–507.

Mascarenhas, M.I., Parker, A., Dzierzak, E., and Ottersbach, K. (2009). Identification of novel regulators of hematopoietic stem cell development through refinement of stem cell localization and expression profiling. Blood *114*, 4645–4653.

McQualter, J.L., Yuen, K., Williams, B., and Bertoncello, I. (2010). Evidence of an epithelial stem/progenitor cell hierarchy in the adult mouse lung. Proc. Natl. Acad. Sci. USA *107*, 1414–1419.

Moore, T., Constancia, M., Zubair, M., Bailleul, B., Feil, R., Sasaki, H., and Reik, W. (1997). Multiple imprinted sense and antisense transcripts, differential methylation and tandem repeats in a putative imprinting control region upstream of mouse Igf2. Proc. Natl. Acad. Sci. USA *94*, 12509–12514.

Park, I.K., Morrison, S.J., and Clarke, M.F. (2004). Bmi1, stem cells, and senescence regulation. J. Clin. Invest. *113*, 175–179.

Park, H.C., Boyce, J., Shin, J., and Appel, B. (2005). Oligodendrocyte specification in zebrafish requires notch-regulated cyclin-dependent kinase inhibitor function. J. Neurosci. *25*, 6836–6844.

Rawlins, E.L., Ostrowski, L.E., Randell, S.H., and Hogan, B.L. (2007). Lung development and repair: contribution of the ciliated lineage. Proc. Natl. Acad. Sci. USA *104*, 410–417.

Rawlins, E.L., Okubo, T., Xue, Y., Brass, D.M., Auten, R.L., Hasegawa, H., Wang, F., and Hogan, B.L. (2009). The role of Scgb1a1+ Clara cells in the long-term maintenance and repair of lung airway, but not alveolar, epithelium. Cell Stem Cell *4*, 525–534.

Sauvageau, M., and Sauvageau, G. (2010). Polycomb group proteins: multi-faceted regulators of somatic stem cells and cancer. Cell Stem Cell *7*, 299–313.

Stadtfeld, M., Apostolou, E., Akutsu, H., Fukuda, A., Follett, P., Natesan, S., Kono, T., Shioda, T., and Hochedlinger, K. (2010). Aberrant silencing of imprinted genes on chromosome 12qF1 in mouse induced pluripotent stem cells. Nature *465*, 175–181.

Terranova, R., Yokobayashi, S., Stadler, M.B., Otte, A.P., van Lohuizen, M., Orkin, S.H., and Peters, A.H. (2008). Polycomb group proteins Ezh2 and Rnf2 direct genomic contraction and imprinted repression in early mouse embryos. Dev. Cell *15*, 668–679.

Umemoto, T., Yamato, M., Nishida, K., Yang, J., Tano, Y., and Okano, T. (2006). Limbal epithelial side-population cells have stem cell-like properties, including quiescent state. Stem Cells *24*, 86–94.

Umlauf, D., Goto, Y., Cao, R., Cerqueira, F., Wagschal, A., Zhang, Y., and Feil, R. (2004). Imprinting along the Kcnq1 domain on mouse chromosome 7 involves repressive histone methylation and recruitment of Polycomb group complexes. Nat. Genet. *36*, 1296–1300.

Varrault, A., Gueydan, C., Delalbre, A., Bellmann, A., Houssami, S., Aknin, C., Severac, D., Chotard, L., Kahli, M., Le Digarcher, A., et al. (2006). Zac1 regulates an imprinted gene network critically involved in the control of embryonic growth. Dev. Cell *11*, 711–722.

Yamazaki, S., Iwama, A., Takayanagi, S., Morita, Y., Eto, K., Ema, H., and Nakauchi, H. (2006). Cytokine signals modulated via lipid rafts mimic niche signals and induce hibernation in hematopoietic stem cells. EMBO J. *25*, 3515–3523.